Noninvasive photoacoustic identification of sentinel lymph nodes containing methylene blue *in vivo* in a rat model

Kwang Hyun Song
Erich W. Stein
Washington University in Saint Louis
Department of Biomedical Engineering
Optical Imaging Laboratory
Campus Box 1097
One Brookings Drive
Saint Louis, Missouri 63130-4899

Julie A. Margenthaler
Washington University School of Medicine
Department of Surgery
660 South Euclid
Campus Box 8109
Saint Louis, Missouri 63110

Lihong V. Wang
Washington University in Saint Louis
Department of Biomedical Engineering
Optical Imaging Laboratory
Campus Box 1097
One Brookings Drive
Saint Louis, Missouri 63130-4899

Abstract. Sentinel lymph node biopsy (SLNB) has become the standard method of axillary staging for patients with breast cancer and clinically negative axillae. Even though SLNB using both methylene blue and radioactive tracers has a high identification rate, it still relies on an invasive surgical procedure with associated morbidity. Axillary ultrasound has emerged as a diagnostic tool to evaluate the axilla, but it can only assess morphology and cannot specifically identify sentinel lymph nodes (SLNs). In this pilot study, we propose a noninvasive photoacoustic SLN identification system using methylene blue injection in a rat model. We successfully image a SLN with high optical contrast (146 ± 41, standard deviation) and good ultrasonic resolution ($\sim 500~\mu$m) *in vivo*. We also show potential feasibility for clinical applications by imaging 20- and 31-mm-deep SLNs in 3-D and 2-D, respectively. Our results suggest that this technology would be a useful clinical tool, allowing clinicians to identify SLNs noninvasively *in vivo*. © 2008 Society of Photo-Optical Instrumentation Engineers. [DOI: 10.1117/1.2976427]

Keywords: sentinel lymph node biopsy; axillary lymph node dissection; methylene blue; noninvasive; photoacoustic imaging.

Paper 08070R received Feb. 28, 2008; revised manuscript received May 28, 2008; accepted for publication May 29, 2008; published online Sep. 15, 2008.

1 Introduction

Sentinel lymph node biopsy (SLNB) has recently emerged as an accurate, less invasive alternative to axillary lymph node dissection (ALND) and has rapidly become the standard of care for patients with clinically node-negative breast cancer.[1,2] In SLNB, lymphatic mapping with radio-labeled sulfur colloid and/or blue dye is used to identify a sentinel lymph node (SLN) that is most likely to contain metastatic breast cancer. Thus, the pathologic status of the axilla can be predicted, but there are a number of practical limitations to SLNB. First, published SLNB identification rates are between 90 to 95%, and the sensitivity of SLNB is between 88 to 95% in experienced hands.[1–3] This limitation results in persistent axillary disease in about 5 to 10% of breast cancer patients, representing the false negative rate. Second, SLNB is often performed as a staged procedure, requiring that breast cancer patients undergo two or more operations for definitive staging and the treatment of the axilla. Such patients include those who have node-positive disease by SLNB and require complete ALND, those who require axillary staging prior to breast reconstruction, and those who are undergoing neoadjuvant chemotherapy. These clinical scenarios represent up to 40 to 50% of patients treated for breast cancer. Last, although SLNB is clearly less invasive than ALND, it is not without morbidity.

A recent randomized prospective trial of SLNB versus ALND confirms that complications of SLNB include seroma formation, lymphedema, sensory nerve injury, and limitation in range of motion.[4] These limitations of SLNB strongly suggest that alternative strategies to stage the axilla should be explored.

Several reports suggest that axillary ultrasound (AUS) is a potentially valuable technique for identifying axillary metastases.[5–7] AUS permits the visualization of lymph node size, shape, contour, and changes in cortical morphology and texture that appear to be associated with the presence of axillary metastases. However, sonographic signs of metastatic disease may overlap with those of benign reactive changes, limiting the ability of this modality alone to stage the axilla accurately. Therefore, an imaging modality that could accurately identify a SLN *in vivo* would allow noninvasive axillary staging, with either percutaneous fine needle aspiration biopsy (FNAB) or other emerging molecular techniques.

Toward this goal, an *in vivo* photoacoustic (PA) imaging modality is proposed to identify a SLN accurately, where methylene blue is accumulated, in a rat model. PA imaging is based on the generation of PA waves by safely depositing short-pulsed optical energy into tissue. Deposited energy causes thermoelastic expansion and generates PA waves.[8–10] PA imaging is a hybrid technology retaining high optical contrast while overcoming the poor spatial resolution of pure optical imaging and providing good spatial resolution by detect-

Address all correspondence to Lihong V. Wang, Washington University in Saint Louis, Department of Biomedical Engineering, Optical Imaging Laboratory, Campus Box 1097, One Brookings Drive, Saint Louis, Missouri 63130-4899, E-mail: lhwang@biomed.wustl.edu
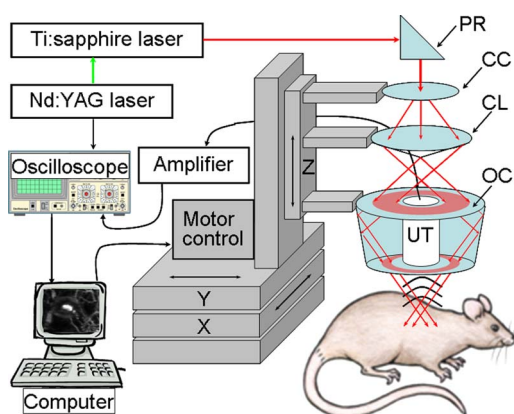
Fig. 1 Schematic of a reflection-mode photoacoustic imaging system. PR, prism; CC, concave lens; CL, conical lens; OC, optical condenser; and UT, ultrasonic transducer.

ing ultrasound, which has relatively low scattering.[11,12] The result of this research suggests that this PA technique may provide an alternative method to localize a SLN accurately.

2 Materials and Methods

2.1 Photoacoustic Imaging

A reflection-mode photoacoustic (PA) imaging system (Fig. 1) was used for identifying a SLN following methylene blue injection. This imaging system employed a dark-field ring-shaped illumination.[13] By reducing the surface PA wave generation, this illumination allows more efficient detection of PA waves from the deep regions, compared with a bright field one. The surface PA waves can interfere with those from deeper regions and obstruct their detection.[13,14] The dark-field illumination was formed by a concave lens, a spherical conical lens, and an optical condenser arranged on an optical rail in tandem. To deliver high optical energy to a deeply located SLN, we used two prisms mounted on an xy linear translation stage instead of an optical fiber, which has lower damage threshold.

For PA excitation, a 635-nm wavelength from a pulsed laser was chosen. This wavelength is close to that of methylene blue's peak optical absorption (677-nm wavelength), which is ten times greater than hemoglobin on a per molar basis (95% oxygenated hemoglobin).[15] The light source was a tunable dye laser (ND6000, Continuum, Santa Barbara, California) pumped by Q-switched Nd:YAG [LS-2137, LOTIS (Minsk, Belarus) II] laser, which provides $<$15-ns pulse duration and a 10-Hz pulse repetition rate. Laser light delivered to the skin was sufficiently broadened by a concave lens to conform to the maximum permissible exposure (MPE) limitation (actual fluence: 3.4 mJ/cm^2, MPE: 20 mJ/cm^2).[16] We chose a 635-nm wavelength, since the dye laser produces maximum energy at this wavelength with a DCM dye.

A 3.5- or 5-MHz central frequency ultrasonic transducer (V380, V308, Panametrics-NDT, Watham, Maryland) was used for the PA signal detection, since ultrasonic waves at these frequencies suffer less acoustic attenuation in tissue than higher frequency waves. Both transducers were spherically focused, and had 4.95- and 2.54-cm focal lengths; 2.54- and 1.91-cm-diam active elements; and 70 and 72% bandwidths

based on the full width at half maximum (FWHM) amplitudes, respectively. Transverse resolution of the system was estimated by $1.22\lambda f/d$ (λ is the measured central wavelength, f is the focal length, and d is the diameter of an active element). Thus, the 5-MHz transducer was more suited for higher transverse resolution imaging than the 3.5-MHz one. The 3.5-MHz transducer was appropriate for deeper imaging, since it has a longer focal length. The spatial resolutions of the system with the 5-MHz ultrasonic transducer at 19 mm deep were $\sim$144 μm in the axial direction and $\sim$560 μm in the transverse direction.[13]

To obtain 3-D PA data, raster scanning was employed using an xy linear translation stage (XY-6060, Danaher Motion, Washington, D. C.). This stage was controlled by a computer and synchronized with the data acquisition system. A continuous scan was used to shorten data-acquisition time without signal averaging. On the other hand, a stop-and-go scan was used to average PA signals to improve their SNR for deeper SLN imaging. The PA signal obtained along the depth direction (z direction) at a single point is called an A-scan. A 2-D B-scan was acquired by a 1-D scan, and was composed of multiple A-scans (x direction). With a 2-D scan (xy directions), a 3-D image was acquired. An A-scan, resolved in time along the depth direction, was converted into a 1-D depth-resolved image by multiplying it by the speed of sound in soft tissues ($\approx$1500 m/s).

Scanning step sizes were $\sim$0.2 and $\sim$0.4 mm for 1-D and 2-D scans, respectively. With 0.1- and 0.2-mm step sizes and a 10-Hz pulse-repetition-frequency laser system, the acquisition time was $\sim$25 sec for a B-scan and $\sim$42 min for a 3-D image, covering a 20×20-mm field of view. The transducer scanned an object through a 5×5-cm opening sealed with a thin, clear membrane in a water container. The opening was located on the bottom of the water container. Ultrasonic gel was used between the clear membrane and the object to couple the ultrasound.

Following amplification by an amplifier (5072PR, Panametrics-NDT), PA signals were digitized by an oscilloscope (TDS 5054, Tektronix, Natham, Massachusetts) with a 50 mega-sampling rate. Since the laser system has pulse-to-pulse fluctuations in energy, PA signals were compensated by the signals from the photodiodes (DET110, Thorlabs, newton, New Jersey), which sample the energy of each laser pulse.

2.2 Samples

Two types of phantom experiments were performed to assess the device's sensitivity and estimate *in vivo* and *ex vivo* the concentration of methylene blue accumulated in a SLN. The PA signal from a SLN was compared with those from phantoms that had known concentrations of methylene blue to measure the concentration in the SLN. First, laboratory tubing (Dow Corning Corporation, Corning, New York) with 1.47-mm inner diameter (ID) was placed between two layers of chicken breast tissue, as depicted in Fig. 2(b). The tubing was filled with methylene blue of concentrations ranging from 0.1 to 1%, in 0.1% increments. The top tissue layer was $\sim$12 and 20 mm thick in two consecutive sets of measurements. The effective attenuation coefficient of chicken breast tissue is $\sim$0.9 cm^{-1} at the 635-nm wavelength, similar to that of human breast tissue.[17,18] PA signals were measured from meth-
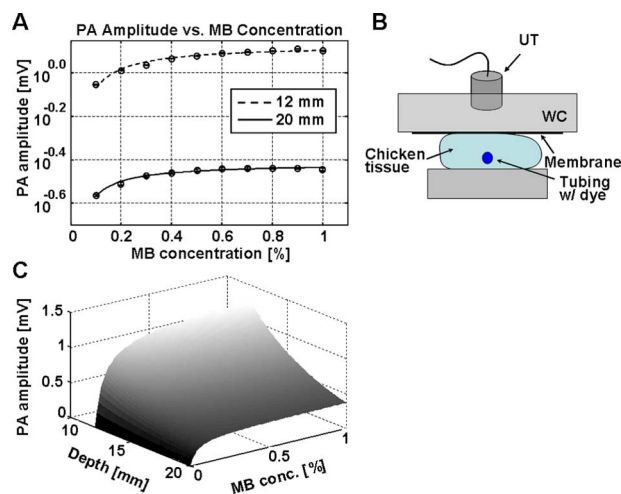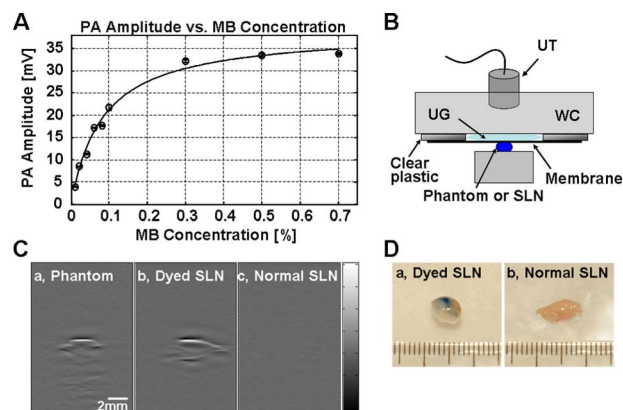
Fig. 2 (a) Amplitude of photoacoustic signal versus concentration of methylene blue dye at 12- and 20-mm depth in chicken breast tissue, respectively. (b) Experimental setup for sensitivity measurement and *in vivo* estimation of concentration. (c) Estimation of concentration at 0- to 20-mm depth. UT, ultrasonic transducer; and WC, water container.

Fig. 3 (A) Amplitude of photoacoustic signal versus concentration of methylene blue dye at a pseudolymph node. (B) Setup for *ex-vivo* estimation of concentration. (C) Photoacoustic B-scans of the phantom, the dyed SLN, and the normal SLN. The concentration in the phantom is ∼0.07%, and the dyed SLN was estimated to be the same concentration. (D) Photographs of SLNs with (left) and without (right) dye deposit. ultrasonic transducer, UG: ultrasonic gel, and Wc: Water container.

ylene blue within the tubing. Before measurement of PA signals at each concentration, the tubing was cleaned with 0.9% saline to remove residual dye. To estimate the *in vivo* concentration of methylene blue, the PA signal from an *in vivo* SLN was compared with that from this phantom experiment. Second, similar to the first case, pseudolymph nodes of comparable dimensions were made of porcine gelatin mixed with methylene blue of various concentrations (0.009 to 0.7%). The pseudolymph node experiments were performed to estimate the concentration of the dye from an excised SLN *ex vivo*. These pseudolymph nodes were cylinders 3 mm in diameter and 4 mm in length, similar to the dimensions of a rat SLN. PA signals were directly measured from these pseudolymph nodes [Fig. 3(b)]. The PA signal from the excised SLN was compared with those from the pseudolymph nodes to estimate the dye concentration. By using comparable dimensions, the effect of the size of the optical absorber was ruled out.

2.3 Animal and Drug Information

All animal experiments were carried out in compliance with the guidelines on the care and the use of laboratory animals at Washington University in Saint Louis. Adult male Sprague Dawley rats weighing 250 to 350 g were used. The rat was initially anesthetized with a mixture of ketamine (85 mg/kg) and xylazine (15 mg/kg). Before imaging, the hair on the region of interest was gently removed using a commercial hair-removal lotion. Intradermal injection of 0.07 ml of 1% methylene blue (10 mg/mL, American Regent, Incorporated) was performed on a left forepaw pad. After administration of methylene blue, photoacoustic images were acquired. During all image acquisitions, anesthesia was maintained using vaporized isoflurane (1-L/min oxygen and 0.75% isoflurane, Euthanex Corporation, Shirley, New York), and vitals were monitored using a pulse oximeter (8600V Nonin Medical Incorporated, Plymouth, Minnesota). During image acquisition,

8 ml of 0.9% saline was administered for hydration. After image acquisition, the animal was euthanized by pentobarbital overdose.

3 Results

3.1 Sensitivity of the System

An imaging system with high sensitivity is required to detect low concentrations of methylene blue accumulated in a SLN located deep below the skin surface. The sensitivity of the photoacoustic (PA) imaging system was obtained from the chicken tissue phantom experiments. Figure 2(a) shows the peak PA signal amplitude versus methylene blue concentration at 12- and 20-mm depths, respectively. The detection limit of the system was calculated to be ∼0.07 mV (three times the standard deviation of the photoacoustic signal without the dye) at 20 mm. This voltage corresponds to a 0.009% concentration based on the extrapolation of the 20-mm curve in (Fig. 2(a)). Therefore, the imaging system is expected to be able to detect a SLN containing greater than 0.009% (0.28-mM) methylene blue located 20 mm from the skin surface. However, the depth capability of the system is not limited to ∼20 mm deep.

### 3.2 Concentration Estimation in Vivo and ex Vivo

To identify a SLN from a group of lymph nodes, it is necessary to measure the concentration of methylene blue accumulated within the SLN. *in vivo* concentration within a SLN can be estimated by measuring a PA signal from the SLN and reading the concentration corresponding to the measured PA signal in Fig. 2(a) at the 12- and 20-mm depth. Since the amplitudes of PA signals are proportional to optical fluence in a medium, and the fluence between two depths can be estimated based on the diffusion equation,[19] the amplitudes of PA signals for other depths were interpolated using the diffusion equation for all concentrations of methylene blue. Interpolated values were plotted in mesh [Fig. 2(c)]. The imaging depth

(~18 mm) was demonstrated by placing two layers of chicken breast tissue on top of the axillary surface of the rat *in vivo*. At this depth, the peak amplitude of the PA signal from the SLN was ~0.3 ± 0.008 mV (standard error), corresponding to ~$0.07\% \pm 0.05\%$ (2.2 mM, standard error) methylene blue [Fig. 2(c)]. For concentrations below 0.1% in (Fig. 2(b)), the amplitudes of the PA signals were extrapolated based on the diffusion equation.

After all *in vivo* PA images of the rat SLN were acquired, the SLN was excised to measure the PA signal more accurately. The peak amplitude of the PA signal, which was acquired using the method depicted in Fig. 3(b), was ~17 ± 0.09 mV (standard error). This voltage corresponds to ~$0.07\% \pm 0.0006\%$ (standard error) methylene blue [Fig. 3(a)], which is equivalent to the *in vivo* estimation at 18-mm depth. These results show that the imaging system has high sensitivity and accuracy in identifying a SLN and in estimating its dye content both *in vivo* and *ex vivo*. [Figure 3(c)] shows the PA B-scans of the pseudolymph node, the dyed SLN, and the normal SLN. The pseudolymph node in Fig. 3(c) "Phantom," had a concentration of ~0.07%, equivalent to that of the dyed SLN in Fig. 3(c) "Dyed SLN." Therefore, both the pseudolymph node and the dyed SLN have PA signals of the same amplitude. By contrast, the normal SLN did not generate a PA signal, showing that this did not exhibit optical contrast. Figure 3(d) shows photographs of a dyed SLN and a normal SLN, respectively. Should this technology be accepted clinically, the average concentration in a SLN can be measured and used for SLN identification.

3.3 Sentinel Lymph Node Imaging in a Rat in Vivo

A rat SLN was clearly imaged by noninvasive *in vivo* PA imaging. Figure 4(a) is a photograph of a rat taken prior to image acquisition and after hair removal of the axillary surface; Fig. 4(b) is a photograph of the same rat with the skin removed after PA imaging. The SLN is unclear in the photograph because it is surrounded by fatty tissue. Before methylene blue injection, a PA control image was obtained, and is shown in the form of a maximum amplitude projection (MAP) [Fig. 4(c)].[20] The vasculature near an axial node was clearly imaged with high contrast (51 ± 7, standard deviation with respect to the background) and good resolution (~500 μm). Since methylene blue molecules are small (0.7 nm in diameter and 1.6 nm in length)[21] and migrate into a SLN quickly, scanning started immediately after administration of methylene blue. The SLN appeared at the left top corner with a much higher contrast (146 ± 41, standard deviation with respect to the background) than the surrounding blood vessels [Fig. 4(d)], since methylene blue has higher optical absorption than blood at the 635-nm wavelength. The contrast of the SLN with respect to the blood vessel was ~2. The signal amplitude of the surrounding blood vessels was also increased by ~$19\% \pm 3\%$ compared to that in the control image, since some of methylene blue flowed into the blood stream directly and/or through the SLN. Accordingly, optical absorption in blood was increased. In all PA images, the brighter the object, the higher the absorption. Another PA image was acquired at ~50 min after dye injection with the scan head repositioned [Fig. 4(e)]. The SLN was still observed. In humans, the mean depth of SLNs is 12 ± 5 mm
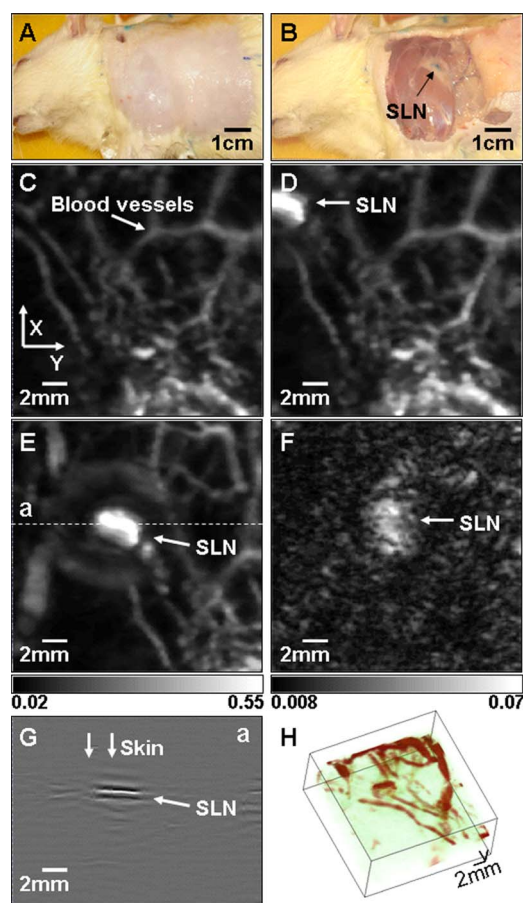
Fig. 4 Noninvasive *in vivo* photoacoustic MAP images of the SLN in a rat. (A) Photograph with hair removed before photoacoustic imaging. (B) Photograph with skin removed after photoacoustic imaging. (C) Control photoacoustic image without methylene blue injection. Bright parts represent optical absorption, here, blood vessels. *x* and *y* denote B-scan and 3-D imaging. (D) After-injection photoacoustic image. (E) After-injection photoacoustic MAP image ~52 min after injection with the scan head repositioned. (F) Photoacoustic MAP image of ~18-mm-deep SLN. Chicken breast tissue was placed on top of the axillary surface of the rat. (G) Photoacoustic B-scan image corresponding to the dotted line in (E), showing the depth of the SLN. The vertical axis in this image corresponds to depth. (H) Photoacoustic 3-D volumetric visualization. The color bars represent optical absorption. (C) and (D) have the same color bar range as (E). (Color online only.)

(standard deviation, from the SLN's top surface to the skin surface (unpublished data), To check the feasibility of this imaging depth, chicken breast tissue was placed on top of the axillary surface of the rat, and then a PA image was obtained [Fig. 4(f)]. The demonstrated imaging depth was ~18 mm. Since methylene blue accumulated in the SLN still had higher absorption than the nearby blood vessels, the SLN is dominant in the PA image, while the blood vessels have faded away. Figure 4(g) shows an image of B-scans along the dotted line in Fig. 4(e), showing the depth of the SLN. A 3-D volumetric image was also constructed [Fig. 4(h)]. In some clinical cases, the depth of a SLN is greater than 18 mm (18 ± 5 mm, standard deviation, from the SLN's bottom surface to the skin surface). To increase imaging depth as well as SNR, higher incident energy of a laser is necessary for the PA
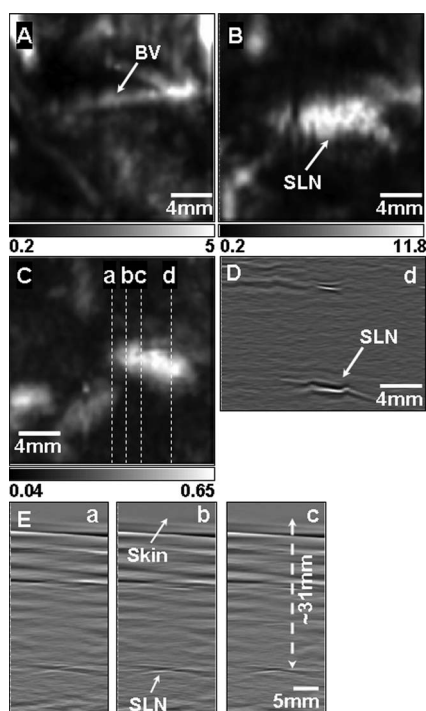
Fig. 5 Noninvasive *in vivo* photoacoustic MAP images of the SLN in another rat. (A) Control photoacoustic image without methylene blue injection. (B) After-injection photoacoustic image. (C) Photoacoustic MAP image of 20-mm-deep SLN. (D) Photoacoustic B-scan image corresponding to the dotted line (d) in (C). (E) Photoacoustic B-scan images acquired at three different locations [(a), (b), (c)] in (C). Total imaging depth was ~31 mm. For this depth, the 3.5-MHz transducer and 50 times averaging were employed.

excitation, while still staying within the MPE. We note that in this study, the incident fluence of the laser was five times less than the MPE, so increasing the laser fluence can enhance the PA signal by five times.

Accordingly, *in vivo* PA SLN imaging of another rat was conducted with twice the incident optical fluence. The 3.5-MHz central frequency ultrasonic transducer (V380, Panametrics-NDT) was employed instead of the 5-MHz one, since the former has a longer focal length and is more suitable for deeper SLN identification. Figure 5(a) is the PA control image before injection of methylene blue, showing vasculature in the skin. [Figure 5(b)] reveals the SLN after methylene blue injection. For demonstration at a greater depth, chicken breast tissue about 18 mm thick was placed on the axillary region. Figure 5(c) is an ~20-mm-deep PA SLN image. In Fig. 5(c), the contrasts of the SLN and the blood vessel with respect to the background were 24.5 ± 3.3 and 13 ± 2.3 (standard deviation), respectively. The contrast of the SLN with respect to the blood vessel was ~0.9. Figure 5(d) is an image of B-scans acquired along the far-right dotted line in Fig. 5(c), showing the depth of the SLN. Here, the skin surface is not shown due to the limited record length of the acquisition system. We further tried deeper SLN imaging by adding a second layer of chicken breast tissue. Three B-scan images [Fig. 5(e)] were obtained at three locations of the SLN area with 50 times averaging. The total imaging depth demonstrated was ~31 mm, greater than the mean depth of the SLN in humans (from the SLN's bottom surface to the skin surface).

4 Discussion

Since this imaging system currently employs a 10-Hz pulse-repetition-frequency laser and a raster scan using a focused ultrasonic transducer, the acquisition times for B-scan and 3-D imaging are limited to about 25 sec with a 100-μm step size and 42 min with a 200-μm step size, respectively. Therefore, employing a higher pulse-repetition-frequency laser, say 50 Hz, and an ultrasound array system can accelerate acquisition, allowing potentially real-time photoacoustic (PA) imaging. The acquisition time can also be reduced by increasing the step sizes. Except for Fig. 5(e), the PA signals were not averaged to shorten the scanning time. With the availability of an ultrasound array system and a higher pulse-repetition-frequency laser, signal averaging can be implemented within a reasonable time frame to improve SNR. In current SLNB practice, two or more surgeries are necessary for the definitive staging and treatment of the axilla. Furthermore, common side effects may be experienced by the patient as previously described. Since PA SLN identification is totally noninvasive and safe, it has potential future applications in the identification of SLNs *in vivo* in clinical practice, thus reducing patient morbidity.

In conclusion, the feasibility of noninvasive SLN identification based on methylene blue injection in an animal model was demonstrated with *in vivo* PA imaging. The proposed imaging system was proven to be highly sensitive (0.28 mM) to methylene blue and suitable to estimate the dye concentration accumulated within a SLN both *in vivo* and *ex vivo* with high optical contrast and good ultrasonic resolution. In addition, a SLN can be located in the *x*, *y*, and *z* directions. With these features, the proposed PA imaging technology offers a potentially minimally invasive method of SLN identification. Future studies may be directed toward the diagnostic sampling of PA-localized SLNs using either percutaneous FNAB and/or molecular techniques, potentially eliminating the need for invasive axillary staging procedures.

References

1. D. Krag, D. Weaver, T. Ashikaga, F. Moffat, V. S. Klimberg, C. Shriver, S. Feldman, R. Kusminsky, M. Gadd, J. Kuhn, S. Harlow, and P. Beitsch, "The sentinel node in breast cancer—a multicenter validation study," *N. Engl. J. Med.* **339**(14), 941–946 (1998).
2. K. M. McMasters, T. M. Tuttle, D. J. Carlson, C. M. Brown, R. D. Noyes, R. L. Glaser, D. J. Vennekotter, P. S. Turk, P. S. Tate, A. Sardi, P. B. Cerrito, and M. J. Edwards, "Sentinel lymph node biopsy for breast cancer: a suitable alternative to routine axillary dissection in multi-institutional practice when optimal technique is used," *J. Clin. Oncol.* **18**(13), 2560–2566 (2000).
3. O. A. Ung, "Australasian experience and trials in sentinel lymph node biopsy: the RACS SNAC trial," *Asian J. Surg.* **27**(4), 284–290 (2004).
4. A. D. Purushotham, S. Upponi, M. B. Klevesath, L. Bobrow, K. Millar, J. P. Myles, and S. W. Duffy, "Morbidity after sentinel lymph node biopsy in primary breast cancer: Results from a randomized controlled trial," *J. Clin. Oncol.* **23**(19), 4312–4321 (2005).
5. B. Brancato, M. Zappa, D. Bricolo, S. Catarzi, G. Risso, R. Bonardi,

P. Cariaggi, A. Bianchin, P. Bricolo, M. Rosselli Del Turco, L. Cataliotti, S. Bianchi, and S. Ciatto, "Role of ultrasound-guided fine needle cytology of axillary lymph nodes in breast carcinoma staging," *Radiol. Med. (Torino)* **108**(4), 345–355 (2004).

6. E. E. Deurloo, P. J. Tanis, K. G. A. Gilhuijs, S. H. Muller, R. Kroger, J. L. Peterse, E. J. T. Rutgers, R. V. Olmos, and L. J. S. Kool, "Reduction in the number of sentinel lymph node procedures by preoperative ultrasonography of the axilla in breast cancer," *Eur. J. Cancer* **39**(8), 1068–1073 (2003).

7. S. Krishnamurthy, N. Sneige, D. G. Bedi, B. S. Edieken, B. D. Fornage, H. M. Kuerer, S. E. Singletary, and K. K. Hunt, "Role of ultrasound-guided fine-needle aspiration of indeterminate and suspicious axillary lymph nodes in the initial staging of breast carcinoma," *Cancer* **95**(5), 982–988 (2002).

8. C. K. N. Patel and A. C. Tam, "Pulsed optoacoustic spectroscopy of condensed matter," *Rev. Mod. Phys.* **53**(3), 517 (1981).

9. C. G. A. Hoelen, F. F. M. de Mul, R. Pongers, and A. Dekker, "Three-dimensional photoacoustic imaging of blood vessels in tissue," *Opt. Lett.* **23**(8), 648–650 (1998).

10. X. Wang, Y. Pang, G. Ku, X. Xie, G. Stoica, and L. V. Wang, "Noninvasive laser-induced photoacoustic tomography for structural and functional in vivo imaging of the brain," *Nat. Biotechnol.* **21**(7), 803–806 (2003).

11. K. H. Song, G. Stoica, and L. V. Wang, "In vivo three-dimensional photoacoustic tomography of a whole mouse head," *Opt. Lett.* **31**(16), 2453–2455 (2006).

12. X. Wang, Y. Pang, G. Ku, X. Xie, G. Stoica, and L. V. Wang, "Noninvasive laser-induced photoacoustic tomography for structural and functional in vivo imaging of the brain," *Nat. Biotechnol.* **21**(7), 803–806 (2003).

13. K. H. Song and L. V. Wang, "Deep reflection-mode photoacoustic imaging of biological tissue," *J. Biomed. Opt.* **12**, 060503 (2007).

14. K. Maslov, G. Stoica, and L. V. H. Wang, "In vivo dark-field reflection-mode photoacoustic microscopy," *Opt. Lett.* **30**(6), 625–627 (2005).

15. S. L. Jacques and S. A. Prahl, "Absorption spectra for biological tissues" (2008).

16. American National Standards and Institute, "American National Standard for the safe use of lasers ANSI Z136.1–2000," New York (2000).

17. G. Marquez, L. H. V. Wang, S. P. Lin, J. A. Schwartz, and S. L. Thomsen, "Anisotropy in the absorption and scattering spectra of chicken breast tissue," *Appl. Opt.* **37**(4), 798–804 (1998).

18. B. J. Tromberg, O. Coquoz, J. Fishkin, T. Pham, E. R. Anderson, J. Butler, M. Cahn, J. D. Gross, V. Venugopalan, and D. Pham, "Noninvasive measurements of breast tissue optical properties using frequency-domain photon migration," *Philos. Trans. R. Soc. London, Ser. B* **352**(1354), 661–668 (1997).

19. L. V. Wang and H. I. Wu, *Biomedical Optics: Principles and Imaging*, Wiley, New York (2007).

20. H. F. Zhang, K. Maslov, G. Stoica, and L. H. V. Wang, "Functional photoacoustic microscopy for high-resolution and noninvasive in vivo imaging," *Nat. Biotechnol.* **24**(7), 848–851 (2006).

21. S. Sohrabnezhad, A. Pourahmad, and M. A. Sadjadi, "New methylene blue incorporated in mordenite zeolite as humidity sensor material," *Mater. Lett.* **61**(11–12), 2311–2314 (2007).